Thermodynamics versus Kinetics Dichotomy in the Linear Self-Assembly of Mixed Nanoblocks

ARTICLE *in* JOURNAL OF PHYSICAL CHEMISTRY LETTERS · MAY 2014

Impact Factor: 7.46 · DOI: 10.1021/jz500776g

2 AUTHORS:

Luis Ruiz
Northwestern University
13 PUBLICATIONS **109** CITATIONS
SEE PROFILE

Sinan Keten
Northwestern University
75 PUBLICATIONS **1,471** CITATIONS
SEE PROFILE

THE JOURNAL OF PHYSICAL CHEMISTRY Letters

Letter

pubs.acs.org/JPCL

Thermodynamics versus Kinetics Dichotomy in the Linear Self-Assembly of Mixed Nanoblocks

L. Ruiz and S. Keten*

Department of Civil & Environmental Engineering and Mechanical Engineering, Northwestern University, Evanston, Illinois 60208-3111, United States

Supporting Information

ABSTRACT: We report classical and replica exchange molecular dynamics simulations that establish the mechanisms underpinning the growth kinetics of a binary mix of nanorings that form striped nanotubes via self-assembly. A step-growth coalescence model captures the growth process of the nanotubes, which suggests that high aspect ratio nanostructures can grow by obeying the universal laws of self-similar coarsening, contrary to systems that grow through nucleation and elongation. Notably, striped patterns do not depend on specific growth mechanisms, but are governed by tempering conditions that control the likelihood of depropagation and fragmentation.

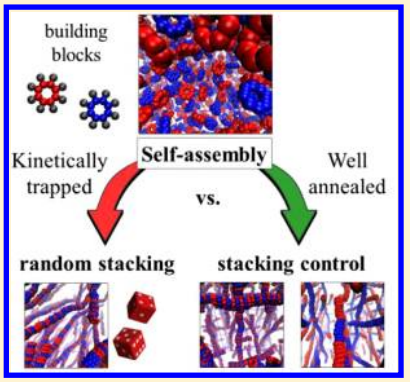

SECTION: Physical Processes in Nanomaterials and Nanostructures

Self-assembly is a low-energy synthesis process, prominent in biological systems, in which smaller building blocks spontaneously associate to form highly organized structures of great complexity.[1−3] Thus, it is one of the most promising strategies to engineer hierarchical functional nanostructures.[4−6] Of special interest are one-dimensional arrays of nanoscale blocks (e.g., nanoparticles, peptides, colloids, etc.), such as nanowires, nanotubes or polymer-like structures, due to their potential applications ranging from nanosensing,[7] optoelectronics,[8] or molecular selective transport[9,10] to mechanical reinforcement in structural composites.[11,12] However, despite considerable advances on the synthesis side in the past few years,[13,14] there is lack of understanding of the physics underlying the self-assembly kinetics and the mixing of diverse building blocks in low-dimensional structures.

Short-term kinetic mechanisms of growth (in the order of nanoseconds to milliseconds) are difficult to reach with computationally intensive molecular simulations, and yet occur too rapidly to be resolved with experiments. Even for widely studied low-dimensional systems such as amyloid forming peptides, short-term kinetics investigations have led to conflicting hypotheses on whether the formation of oligomers at early times is negligible (the nucleated polymerization mechanism[15]), or otherwise significant (the nucleated conformational conversion mechanism[16]). The growth mechanisms and kinetics of structurally analogous systems such as peptide nanotubes[17] remain unexplored.

Regarding supramolecular organization, previous studies have illustrated that subunit anisotropy and entropic effects alone can strongly influence the resulting configuration.[18−23] However, the effect of kinetic traps on the formation of arrested phases is not yet fully understood, particularly in systems where self-assembly is driven by enthalpic interactions and non-equilibrium configurations are prevalent.[24−27]

As a model system representative of the main features of high-aspect ratio assemblies, namely, anisotropic geometry and favorable short-range interactions, we study binary mixtures of small nanorings (∼1 nm in diameter) that self-assemble into nanotubes (Figure 1). Our work is inspired by recent experiments on cyclic peptide nanotubes (CPNs)[28] and other macrocycles,[29] where the binding energies between different units can be finely tuned through enthalpic as well as entropic contributions arising from polymer conjugation, solvents, and peptide chemistry (Figure 1a).[30] In our molecular model (Figure 1), we use rings that have eight backbone beads each, all of which are either type A or B. The backbone beads interact through a Lennard-Jones potential[31] with energy parameters ε_{AA}, ε_{AB}, and ε_{BB}, where $\varepsilon_{AA} > \varepsilon_{BB}$ and $\varepsilon_{AA} \geq \varepsilon_{AB} \geq \varepsilon_{BB}$. We use the nondimensional parameter $\chi^* = [(\varepsilon_{AA} + \varepsilon_{BB})/2 - \varepsilon_{AB}]/\Delta\varepsilon$, where $\Delta\varepsilon = \varepsilon_{AA} - \varepsilon_{BB}$, as a measurement of the cross-interactions, and we consider three possibilities: (1) $\varepsilon_{AB} = \varepsilon_{AA}$ or $\chi^* = -0.5$, (2) $\varepsilon_{AB} = (\varepsilon_{AA} + \varepsilon_{BB})/2$ or $\chi^* = 0$, and (3) $\varepsilon_{AB} = \varepsilon_{BB}$ or $\chi^* = 0.5$. The simple nature of our model provides broad insight into linear self-assembly of ring/plate/disk type of nanoblocks that form patterned surfaces and have use in a myriad of technological applications. Further details regarding

Received: April 17, 2014
Accepted: May 8, 2014
Published: May 8, 2014

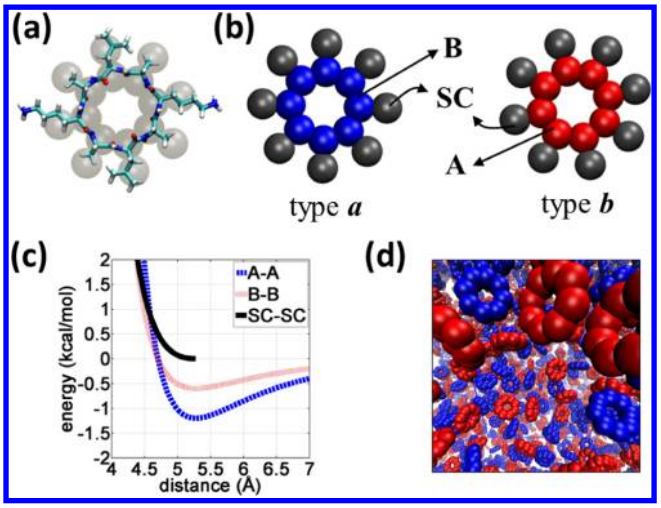

Figure 1. Simulation setup and model schematics. (a) Superposition of the coarse-grain model and an atomistic representation of a cyclic peptide. (b) Each building block is composed of 16 beads (one backbone bead and one side chain bead per amino acid in the cyclic peptide analogy). The side chain beads (type SC) are the same type for all the subunits, but there are two types of backbone beads: A (blue) and B (red). (c) Pairwise interaction potentials (Lennard-Jones functional form) between the different bead types. The SC−A and SC−B interactions are identical to SC−SC (black line) and are purely repulsive. The interactions between the backbone beads, A−A, B−B, and A−B are varied in each case. (d) Snapshot from a simulation at the end of the randomization stage. For clarity in the representation, the side-chain beads are not shown, and periodic images have been added to the sides of the simulation box.

the molecular model and the simulation settings are provided in the Supporting Information.

In this letter, we first analyze the growth kinetics and self-assembly mechanisms of the nanotubes using classical MD simulations. For the kinetic analysis, we keep track of the number of monomers n_{free}, the number of nanotubes, n_{NT}, and the average number of rings in the nanotubes $\langle N \rangle$. For n_{NT}, only dimers or greater aggregation numbers are considered formed nanotubes. The results of the kinetic analysis are shown in Figure 2.

The earlier times of the simulation are characterized by a quick reduction of the number of monomers. During this period, the nanotubes grow by condensation of monomers into dimers and trimers, and the number of nanotubes consequently increases. However, as the monomers get depleted, the growth mechanism of the nanotubes shifts from a condensation governed regime to a period governed by the coalescence of nanotubes. This scenario, where the monomers get depleted and are not replenished, is representative of in vitro experiments in which a given amount of monomers is introduced in a closed system.[32] The availability of monomers can affect the growth mechanisms, where continuous supply of monomers into the solution may prohibit the onset of depletion and thus self-similar coarsening. The coalescence mechanism observed in the simulations is analogous to self-similar coarsening, and therefore we hypothesize that it must follow the kinetics of a self-catalyzed step-growth polymerization (SGP) process (dashed gray curves in Figure 2).[33] This growth mechanism is distinctly different from the nucleation-elongation driven growth (e.g., the nucleated polymerization mechanism) commonly assumed for other one-dimensional

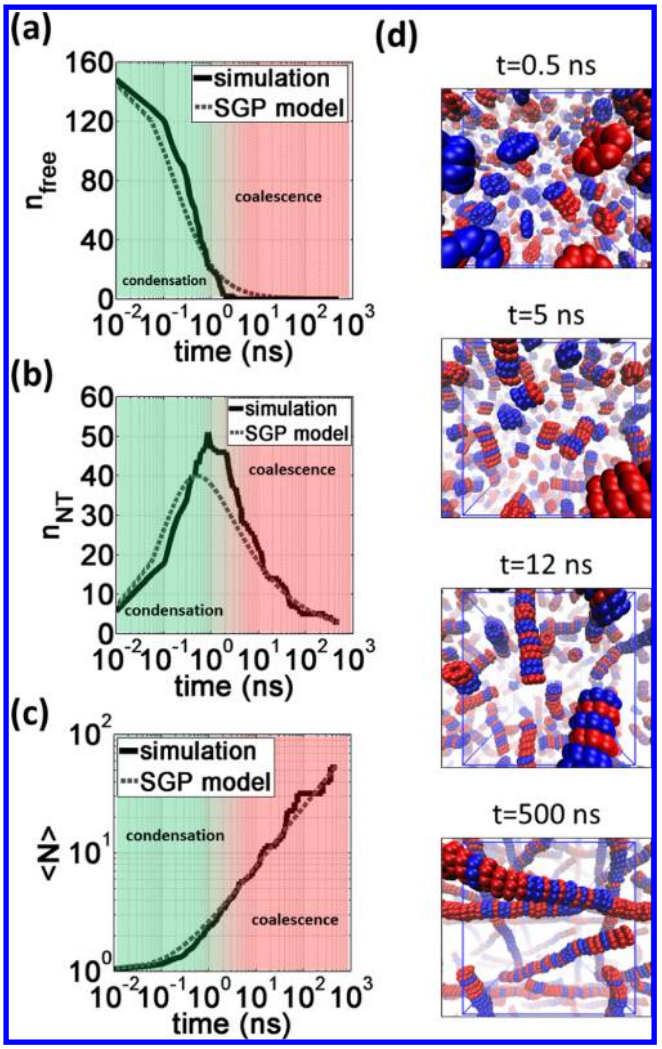

Figure 2. Self-assembly kinetics of the nanotubes. The data represented in this figure corresponds to a classical molecular dynamics simulation (MD), in particular ε_{AA} = 0.8, ε_{BB} = 1.0, and ε_{AB} = 0.9(χ^* = 0). All cases studied exhibit similar self-assembly kinetics. Panels a−c show both the data from the simulations (solid black lines) and best fit curves based on the SGP model (dashed gray lines). (a) The number of monomers as a function of time dramatically decreases ($n_{free} \sim t^{-1}$) up to total depletion in the first ∼2 ns. (b) The number of nanotubes initially grows with time during condensation into oligomers but then decreases due to coalescence of the existing oligomers into large nanotubes. (c) The average aggregation number of nanotubes as a function of time scales linearly as $\langle N \rangle \sim t$ for short time-scales, but generally follows a power law $\langle N \rangle \sim t^{1/2}$, a signature of step-growth polymerization. (d) Time sequence of snapshots from an MD simulation illustrating the growth of the nanotubes. For clarity in the representation, the side-chain beads are not shown, and periodic images have been added to the sides of the simulation box.

supramolecular systems such as protein fibrils.[34] The relevant equations of the SGP model regarding our kinetic variables are

$$\langle N \rangle = (1 + C_1 t)^{1/2} \tag{1}$$

$$n_{free} = \frac{n_{free}^{t=0}}{\langle N \rangle^2} = \frac{n_{free}^{t=0}}{(1 + C_1 t)} \tag{2}$$

$$n_{NT} = \frac{n_{free}^{t=0}}{\langle N \rangle} - n_{free} = \frac{n_{free}^{t=0}[(1 + C_1 t)^{1/2} - 1]}{(1 + C_1 t)} \tag{3}$$

dx.doi.org/10.1021/jz500776g | J. Phys. Chem. Lett. 2014, 5, 2021−2026

where $n_{free}^{t=0}$ is the initial number of monomers, and $C_1 = 2k_u[C_0]^2$ is a constant that depends on the rate constant of the reaction (e.g., dimerization) k_u, and the initial concentration of monomers $[C_0]$. Further details regarding the SGP model formulation and the derivation of eqs 1, 2, and 3 have been provided in the Supporting Information. The time scale of the self-assembly process depends on the constant C_1. For example, if we define the self-assembly characteristic time, t_c, as the time at which the number of nanotubes becomes maximum, $t_c = t(n_{NT}^{max})$, which we can calculate from the condition $dn_{NT}/dt = 0$, we obtain a simple scaling relationship between the initial concentration and the time-scale of growth: $t_c \sim 1/C_1$, or equivalently, $t_c \sim [C_0]^{-2}$. In simulation, the initial concentration is on the order of millimolar and self-assembly occurs in nanoseconds, whereas in experiments, identical mechanisms and phenomena would occur in milliseconds due to the much lower concentrations (in the order of micromolar).

Scaling relationships obtained from the SGP model support the hypothesis that the growth mechanism is self-similar coarsening. For short time-scales, $\lim_{t\to 0}(d\langle N\rangle/dt) =$ constant, suggesting a linear scaling $\langle N\rangle_{t\to 0} \sim t$ that agrees with the growth observed in the simulations during the condensation regime. For longer times, the asymptotic limit of eq 1 becomes $\lim_{t\to\infty} \langle N\rangle \sim t^{1/2}$, which is in accordance with the scaling observed during the coalescence regime.

Despite that step-growth is a well-established polymerization process; it has only been scarcely related to low-dimensional supramolecular assemblies with large persistence length. Some examples of self-assembled systems growing by self-similar coarsening include linear aggregation of inorganic nanoparticles[35] and also in drying-mediated nanoparticle self-assembly.[36,37] The crossover between the growth mechanisms described above (from monomer condensation to nanotube coalescence) is similar to those observed in thin films, where the growth of islands by monomer condensation usually precludes an island coalescence regime.[38] Additionally, our simulations suggest the formation of oligomers at short times and the absence of a nucleation stage. Our molecular model based on CPNs is not designed to be representative of amyloids;[39] however, growth into high-aspect ratio assemblies by beta-sheet formation, similarly to our nanotubes, is a common feature of these systems.[17] Thus, our analysis on the growth kinetics of the nanotubes may shed some light into the short-time kinetics of amyloid formation, supporting the nucleated conformational conversion mechanism (NCC) that proposes significant concentration of oligomers at earlier times,[16] opposed to the nucleation-polymerization model (NP) that assumes a nucleation stage where the concentration of oligomers is negligible at short times. In our simulations the absence of a nucleation stage can be attributed to two factors. First, there is no energetic barrier to the formation of small aggregates (growth is thermodynamically favorable from the start). And second, a conformational transition of the oligomers is not required to enable further growth of the nanotubes from the oligomeric state. Also, energetic barriers to aggregation are absent independently of the concentration of nanorings, so no differences of growth mechanisms with concentration are expected.

In order to achieve functionality through supramolecular structures, it is often necessary to control the spatial organization of the different functional subunits in the structure. In a recent thermodynamic study on binary nanotubes, we hypothesized that the striped pattern of the nanotubes (characterized by the percentage of a−b subunit interfaces n_{ab} in the nanotube) is mainly governed by the value of the intermolecular interaction between dissimilar subunit types (characterized by ε_{AB}) with respect to the homomeric interactions (ε_{AA}, ε_{BB}, where $\varepsilon_{AA} > \varepsilon_{BB}$).[30] The following limiting scenarios were predicted under the assumption of thermodynamic equilibrium. For $\chi^* \approx -0.5$, the nanotubes tend to stack in an alternating fashion ($n_{ab} \approx 100\%$). For $\chi^* \approx 0.5$, the nanotubes tend to form segregated domains ($n_{ab} \approx 0\%$). For the critical case of $\chi^* \approx 0$, the configuration of the subunits is mainly governed by the entropy of mixing and thus the final striped pattern results to be random ($n_{ab} \approx 50\%$).[30] Additionally, based on equilibrium thermodynamics concepts, larger differences between the binding energies, $\Delta\varepsilon = \varepsilon_{AA} - \varepsilon_{BB}$, should lead to stronger tendencies of the systems to adopt the corresponding thermodynamic state.

Here we put this hypothesis to the test by explicitly simulating the self-assembly process of binary nanotubes. We first perform classical MD simulations and quantify the converged values n_{ab} at the end of each simulation (Figure 3a).

We observe that for lower values of $\Delta\varepsilon$, (e.g., $\Delta\varepsilon = 0.4$ or $\Delta\varepsilon = 0.2$), the striped pattern corresponds to a random mixture ($n_{ab} \approx 40-60\%$) and it does not vary much regardless of the value of ε_{AB}. The striped pattern from the simulations tends slightly more toward the thermodynamic prediction for $\Delta\varepsilon = 0.6$. Overall, classical MD cannot reproduce the thermodynamic predictions of the striped patterns. Since the self-assembly process is diffusion-limited, the probability of a monomer to bind to the same or different type of monomer is equal at equal concentrations. This leads to small oligomers with random striped patterns. As these aggregates start to coalesce, the resulting nanotubes conserve the random striped pattern because no depropagation or fragmentation of the nanotubes occurs during the MD simulations at room temperature. This makes it impossible for the rings in the nanotubes to rearrange and attain the global minimum energy pattern, and therefore the nanotubes become kinetically trapped in a random striped pattern. This shortcoming of classical MD has been previously observed in other systems with rugged free energy landscapes, such as protein folding, where the system can get trapped in a local metastable state and it is unable to properly sample the phase space in search for the absolute minimum.[43] In order to enhance the sampling of the phase space, we use replica exchange (REX) molecular dynamics, where multiple replicas of the system are run simultaneously at different temperatures and allowed to exchange via a Monte Carlo algorithm.[40] The access of the system to high temperatures opens the possibility of nanotube rearrangement by depropagation and fragmentation, and thereby enables the escape of the system from kinetic traps. Unlike classical MD, we find that REX simulations yield nanotubes with configurations that are very close to the thermodynamic equilibrium prediction for all cases studied, especially for higher $\Delta\varepsilon$ (Figure 3b). In order to get a holistic picture of the resultant configurations, we reconstruct the phase diagrams of the striped pattern of the nanotubes, n_{ab}, as a function of the intermolecular interactions ($\Delta\varepsilon$ and χ^*) and the tempering conditions (MD vs REX) (Figure 4).

The phase diagrams clearly expose the differences between the tempering conditions, revealing the inadequacy of MD for predicting phases in thermodynamic equilibrium. This suggests that binary low-dimensional assemblies governed by enthalpic interactions are prone to fall into kinetically arrested states corresponding to a random striped pattern of functional

dx.doi.org/10.1021/jz500776g | J. Phys. Chem. Lett. 2014, 5, 2021−2026

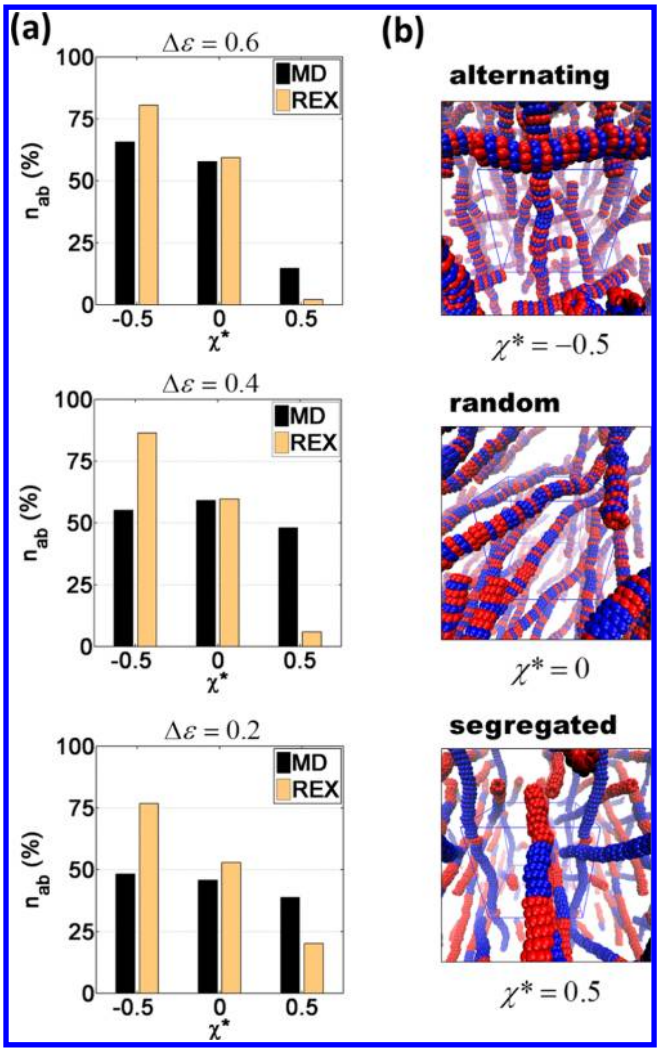

Figure 3. Comparison between REX and classical MD simulation results of the nanotubes striped pattern. (a) Bar plots of the percentage of a−b interfaces for the different cases studied. The MD simulations mostly result in randomly mixed nanotubes ($n_{ab} \approx 40-60\%$), while the REX results are consistent with the thermodynamic equilibrium predictions ($n_{ab} = 100\%$ for $\chi^* = -0.5$, $n_{ab} = 50\%$ for $\chi^* = 0$, and $n_{ab} = 0\%$ for $\chi^* = 0.5$). (b) Snapshots of the observed striped patterns: alternating ($n_{ab} \approx 100\%$), random ($n_{ab} \approx 50\%$), and segregated ($n_{ab} \approx 0\%$) corresponding to the last frame of the REX simulations with $\varepsilon_{AA} = 1.2$ and $\varepsilon_{BB} = 0.6$. For clarity in the representation, the side-chain beads are not shown and periodic images have been added to the sides of the simulation box.

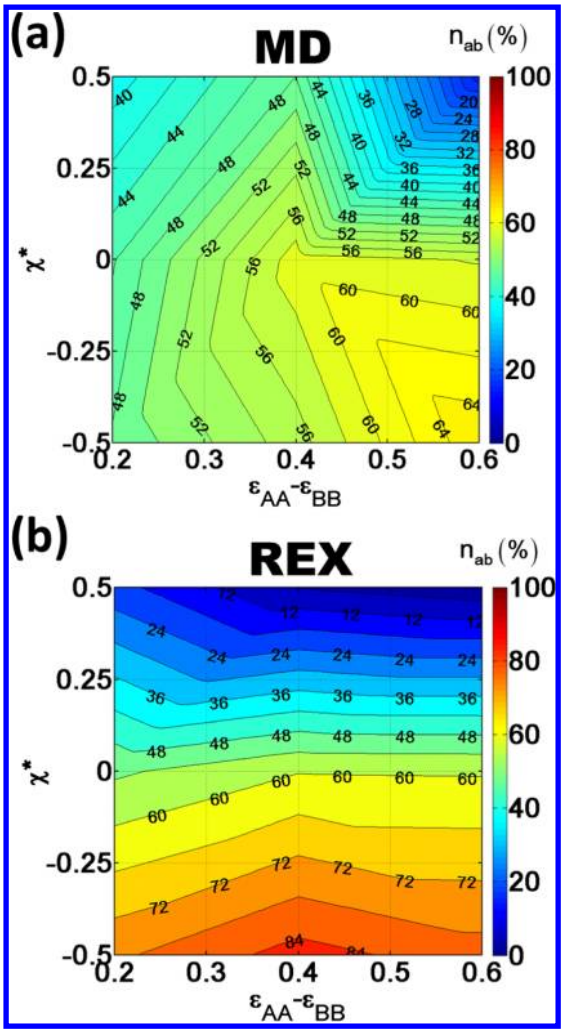

Figure 4. Phase diagrams of the nanotube striped pattern (n_{ab}) as a function of intermolecular interaction parameters ($\Delta\varepsilon$ and χ^*). (a) MD simulation results. The striped pattern does not agree with the thermodynamic prediction and exhibits little variation throughout the parameter space, a clear indication of a kinetically arrested self-assembly process. Only for large values of $\Delta\varepsilon$ the MD simulated systems start to adopt the patterns corresponding to thermodynamic equilibrium (n_{ab} =100% for $\chi^* = -0.5$, $n_{ab} = 50\%$ for $\chi^* = 0$ and $n_{ab} = 0\%$ for $\chi^* = 0.5$). (b) REX simulation results. The striped patterns resulting are in good agreement with the thermodynamic prediction.

subunits. These phase diagrams show the bias of simulation protocols toward particular configurations, and also explain how striped patterns can be tailored by using kinetic and thermodynamic effects concertedly in experiments. Our simulations indicate that annealing conditions as well as intermolecular interactions between the subunits must be controlled to predict self-assembly outcomes.[41,42]

In summary, we have shown that supramolecular nanotubes grow by self-similar coarsening and that this growth mechanism can be described analytically using a step-growth polymerization model. This finding is in clear contrast with the nucleation-elongation growth mechanism commonly assumed for similar low-dimensional systems such as amyloids. In this Letter, we have also shown that kinetic factors associated with tempering conditions along with enthalpic interactions govern the striped patterns of binary nanotubes. In the absence of reversibility mechanisms such as depropagation or fragmentation (e.g., in classical MD simulations), the nanotubes become kinetically trapped in a random striped pattern that is independent of the intermolecular interactions. However, when the nanotubes are allowed to rearrange through the aforementioned reversibility mechanisms (e.g., in REX simulations, Figure S2), the nanotubes were able to adopt the thermodynamically favorable striped patterns that are solely determined by the enthalpic interactions. We anticipate that our predictions, due to the highly generic character of our coarse grain molecular model, could be extrapolated to other systems of colloidal particles that self-assemble into linear aggregates.

dx.doi.org/10.1021/jz500776g | J. Phys. Chem. Lett. 2014, 5, 2021−2026

■ ASSOCIATED CONTENT

Supporting Information

Details regarding the computational model and settings of the simulations are provided in the Supporting Information. This material is available free of charge via the Internet at http://pubs.acs.org.

■ AUTHOR INFORMATION

Corresponding Author

*E-mail: s-keten@northwestern.edu.

Notes

The authors declare no competing financial interest.

■ ACKNOWLEDGMENTS

We are grateful to Dr. Ting Xu for fruitful discussions. This work is supported by the National Science Foundation (DMREF award #CBET-1234305). The authors also acknowledge a supercomputing grant from Northwestern University High Performance Computing Center.

■ REFERENCES

(1) Whitesides, G. M.; Mathias, J. P.; Seto, C. T. *Molecular Self-Assembly and Nanochemistry: A Chemical Strategy for the Synthesis of Nanostructures*; DTIC Document, 1991.

(2) Lehn, J. M. Toward Complex Matter: Supramolecular Chemistry and Self-Organization. *Proc. Natl. Acad. Sci. U. S. A.* **2002**, *99*, 4763−4768.

(3) Moffitt, M. G. Self-Assembly of Polymer Brush-Functionalized Inorganic Nanoparticles: From Hairy Balls to Smart Molecular Mimics. *J. Phys. Chem. Lett.* **2013**, *4*, 3654−3666.

(4) Danial, M.; Tran, C. M.; Young, P. G.; Perrier, S.; Jolliffe, K. A. Janus Cyclic Peptide−Polymer Nanotubes. *Nat. Commun.* **2013**, *4*, 2780.

(5) Ikkala, O.; ten Brinke, G. Functional Materials Based on Self-Assembly of Polymeric Supramolecules. *Science* **2002**, *295*, 2407−2409.

(6) Zhang, S. G. Fabrication of Novel Biomaterials through Molecular Self-Assembly. *Nat. Biotechnol.* **2003**, *21*, 1171−1178.

(7) Anker, J. N.; Hall, W. P.; Lyandres, O.; Shah, N. C.; Zhao, J.; Van Duyne, R. P. Biosensing with Plasmonic Nanosensors. *Nat. Mater.* **2008**, *7*, 442−453.

(8) Maier, S. A.; Kik, P. G.; Atwater, H. A.; Meltzer, S.; Harel, E.; Koel, B. E.; Requicha, A. A. Local Detection of Electromagnetic Energy Transport Below the Diffraction Limit in Metal Nanoparticle Plasmon Waveguides. *Nat. Mater.* **2003**, *2*, 229−232.

(9) Hourani, R.; Zhang, C.; van der Weegen, R.; Ruiz, L.; Li, C.; Keten, S.; Helms, B. A.; Xu, T. Processable Cyclic Peptide Nanotubes with Tunable Interiors. *J. Am. Chem. Soc.* **2011**, *133*, 15296−15299.

(10) Xu, T.; Zhao, N.; Ren, F.; Hourani, R.; Lee, M. T.; Shu, J. Y.; Mao, S.; Helms, B. A. Subnanometer Porous Thin Films by the Co-Assembly of Nanotube Subunits and Block Copolymers. *ACS Nano* **2011**, *5*, 1376−1384.

(11) Rubin, D. J.; Nia, H. T.; Desire, T.; Nguyen, P. Q.; Gevelber, M.; Ortiz, C.; Joshi, N. S. Mechanical Reinforcement of Polymeric Fibers through Peptide Nanotube Incorporation. *Biomacromolecules* **2013**, *14*, 3370−3375.

(12) Sayar, M.; Stupp, S. I. Assembly of One-Dimensional Supramolecular Objects: From Monomers to Networks. *Phys. Rev. E: Stat., Nonlinear, Soft Matter Phys.* **2005**, *72*, 011803.

(13) Palmer, L. C.; Stupp, S. I. Molecular Self-Assembly into One-Dimensional Nanostructures. *Acc. Chem. Res.* **2008**, *41*, 1674−1684.

(14) Hilmer, A. J.; Bellisario, D. O.; Shimizu, S.; McNicholas, T. P.; Wang, Q. H.; Speakman, S. A.; Strano, M. S. Formation of High-Aspect-Ratio Helical Nanorods via Chiral Self-Assembly of Full-erodendrimers. *J. Phys. Chem. Lett.* **2014**, *5*, 929−934.

(15) Xue, W. F.; Homans, S. W.; Radford, S. E. Systematic Analysis of Nucleation-Dependent Polymerization Reveals New Insights into the Mechanism of Amyloid Self-Assembly. *Proc. Natl. Acad. Sci. U. S. A.* **2008**, *105*, 8926−8931.

(16) Serio, T. R.; Cashikar, A. G.; Kowal, A. S.; Sawicki, G. J.; Moslehi, J. J.; Serpell, L.; Arnsdorf, M. F.; Lindquist, S. L. Nucleated Conformational Conversion and the Replication of Conformational Information by a Prion Determinant. *Science* **2000**, *289*, 1317−1321.

(17) Ghadiri, M. R.; Granja, J. R.; Milligan, R. A.; McRee, D. E.; Khazanovich, N. Self-Assembling Organic Nanotubes Based on a Cyclic Peptide Architecture. *Nature* **1993**, *366*, 324−327.

(18) Damasceno, P. F.; Engel, M.; Glotzer, S. C. Predictive Self-Assembly of Polyhedra into Complex Structures. *Science* **2012**, *337*, 453−457.

(19) Bishop, K. J.; Wilmer, C. E.; Soh, S.; Grzybowski, B. A. Nanoscale Forces and Their Uses in Self-Assembly. *Small* **2009**, *5*, 1600−1630.

(20) Horsch, M. A.; Zhang, Z.; Glotzer, S. C. Self-Assembly of Laterally-Tethered Nanorods. *Nano Lett.* **2006**, *6*, 2406−2413.

(21) Iacovella, C. R.; Horsch, M. A.; Zhang, Z.; Glotzer, S. C. Phase Diagrams of Self-Assembled Mono-Tethered Nanospheres from Molecular Simulation and Comparison to Surfactants. *Langmuir* **2005**, *21*, 9488−9494.

(22) Tkachenko, A. V. Theory of Programmable Hierarchic Self-Assembly. *Phys. Rev. Lett.* **2011**, *106*, 255501.

(23) Guo, R. H.; Liu, Z. Y.; Xie, X. M.; Yan, L. T. Harnessing Dynamic Covalent Bonds in Patchy Nanoparticles: Creating Shape-Shifting Building Blocks for Rational and Responsive Self-Assembly. *J. Phys. Chem. Lett.* **2013**, *4*, 1221−1226.

(24) Di Michele, L.; Varrato, F.; Kotar, J.; Nathan, S. H.; Foffi, G.; Eiser, E. Multistep Kinetic Self-Assembly of DNA-Coated Colloids. *Nat. Commun.* **2013**, *4*, 2007.

(25) Hagan, M. F.; Elrad, O. M.; Jack, R. L. Mechanisms of Kinetic Trapping in Self-Assembly and Phase Transformation. *J. Chem. Phys.* **2011**, *135*, 104115.

(26) Whitelam, S.; Schulman, R.; Hedges, L. Self-Assembly of Multicomponent Structures in and out of Equilibrium. *Phys. Rev. Lett.* **2012**, *109*, 265506.

(27) Yin, P.; Choi, H. M.; Calvert, C. R.; Pierce, N. A. Programming Biomolecular Self-Assembly Pathways. *Nature* **2008**, *451*, 318−322.

(28) Couet, J.; Biesalski, M. Polymer-Wrapped Peptide Nanotubes: Peptide-Grafted Polymer Mass Impacts Length and Diameter. *Small* **2008**, *4*, 1008−1016.

(29) Zang, L.; Che, Y.; Moore, J. S. One-Dimensional Self-Assembly of Planar Pi-Conjugated Molecules: Adaptable Building Blocks for Organic Nanodevices. *Acc. Chem. Res.* **2008**, *41*, 1596−1608.

(30) Ruiz, L.; Keten, S. Directing the Self-Assembly of Supra-Biomolecular Nanotubes Using Entropic Forces. *Soft Matter* **2014**, *10*, 851−861.

(31) Jones, J. E. On the Determination of Molecular Fields. I. From the Variation of the Viscosity of a Gas with Temperature. *Proc. R. Soc. A* **1924**, *106*, 441−462.

(32) Castelnovo, M.; Verdier, T.; Foret, L. Comparing Open and Closed Molecular Self-Assembly. *Europhys. Lett.* **2014**, *105*, 28006.

(33) Flory, P. J. *Principles of Polymer Chemistry*; Cornell University Press: Ithaca, NY, 1953.

(34) Wurthner, F. Supramolecular Polymerization: Living It Up. *Nat. Chem.* **2014**, *6*, 171−173.

(35) Liu, K.; Nie, Z.; Zhao, N.; Li, W.; Rubinstein, M.; Kumacheva, E. Step-Growth Polymerization of Inorganic Nanoparticles. *Science* **2010**, *329*, 197−200.

(36) Ge, G. L.; Brus, L. Evidence for Spinodal Phase Separation in Two-Dimensional Nanocrystal Self-Assembly. *J. Phys. Chem. B* **2000**, *104*, 9573−9575.

(37) Tang, J.; Ge, G.; Brus, L. E. Gas−Liquid−Solid Phase Transition Model for Two-Dimensional Nanocrystal Self-Assembly on Graphite. *J. Phys. Chem. B* **2002**, *106*, 5653−5658.

(38) Venables, J. A.; Spiller, G. D. T.; Hanbucken, M. Nucleation and Growth of Thin-Films. *Rep. Prog. Phys.* **1984**, *47*, 399−459.

(39) Bellesia, G.; Shea, J.-E. Self-Assembly of B-Sheet Forming Peptides into Chiral Fibrillar Aggregates. *J. Chem. Phys.* **2007**, *126*, 245104.
(40) Sugita, Y.; Okamoto, Y. Replica-Exchange Molecular Dynamics Method for Protein Folding. *Chem. Phys. Lett.* **1999**, *314*, 141−151.
(41) Winfree, E.; Liu, F.; Wenzler, L. A.; Seeman, N. C. Design and Self-Assembly of Two-Dimensional DNA Crystals. *Nature* **1998**, *394*, 539−544.
(42) Zeng, H.; Li, J.; Liu, J. P.; Wang, Z. L.; Sun, S. Exchange-Coupled Nanocomposite Magnets by Nanoparticle Self-Assembly. *Nature* **2002**, *420*, 395−398.
(43) Keten, S.; Buehler, M. Nanostructure and Molecular Mechanics of Spider Dragline Silk Protein Assemblies. *J. R. Soc. Interface.* **2010**, *7*, 1709−1721.